Journal of The
Electrochemical Society

Enhanced Electrocatalytic Oxidation of Formic Acid on Au(111) in the Presence of Pyridine

To cite this article: Johannes M. Hermann *et al* 2018 *J. Electrochem. Soc.* **165** J3192

JES Focus Issue on Electrocatalysis — In Honor of Radoslav Adzic

Enhanced Electrocatalytic Oxidation of Formic Acid on Au(111) in the Presence of Pyridine

Johannes M. Hermann, Yannick Mattausch, Annchristin Weiß, Timo Jacob, and Ludwig A. Kibler *,z

Institute of Electrochemistry, Ulm University, 89081 Ulm, Germany

The adsorption of pyridine on Au(111) single crystal electrodes has been systematically studied in a broad range of pH values between 1 and 13. From the voltammetric features of Au(111) in 0.1 M pyridine a potential/pH diagram has been derived, which classifies various phases for adsorbed pyridine. At sufficiently high concentrations of unprotonated pyridine in solution, a significantly enhanced activity for formic acid oxidation on Au(111) is observed in a narrow potential region, where strongly bound formate has not yet reached its saturation coverage. The various pyridine structures exhibit different enhancement factors. At positive potentials, the typical features of formic acid oxidation on Au(111) are present, pointing toward complete replacement of adsorbed pyridine by formate.

 [DOI: 10.1149/2.0251815jes]

Manuscript submitted August 16, 2018; revised manuscript received September 25, 2018. Published October 6, 2018. *This paper is part of the JES Focus Issue on Electrocatalysis — In Honor of Radoslav Adzic.*

The advent of electrochemical surface science[1,2] is strongly related with the use of well-ordered single-crystal surfaces, since most electrocatalytic reactions obey a distinct structure-sensitivity.[3] Hence, one-component-catalysts can be optimized by increasing the number of the most active catalytic centers and by increasing the electrochemically active surface area. Furthermore, the design of catalytically active materials crucially depends on various effects of enhancement. In the special case of formic acid oxidation (FAO) on Pt electrodes, electrocatalysis by foreign monolayers has been utilized to suppress the formation of poisonous carbon monoxide.[4,5] Although CO poisoning is practically absent for FAO on Pd and Au,[6] there are still possibilities to boost their electrocatalytic activities. This can be achieved for example by lateral surface strain[7,8] or by adding particular organic molecules to the electrolyte such as pyridine to promote FAO on Au(111), which is the topic of the present paper.

Active sites for FAO on Au(111) are easily blocked by adsorption of spectator species, such as phosphates[9], sulfates[10] and strongly bound formate,[11] which is easily formed from HCOOH or $HCOO^-_{(aq)}$ itself, resulting in a bidentate adsorption configuration. The suppression of strongly bound formate is therefore considered a promising strategy for catalytic enhancement of FAO on Au(111), so that formate is rather adsorbed in a more weakly bounded and reactive configuration.

The adsorption of pyridine has extensively been studied for Au(111) by electrochemical[12–14] and spectroscopic[15–18] methods as well as by in-situ scanning tunneling microcopy (in-situ STM).[15,19] Briefly, adsorption in two different orientations has been reported. A flat and a vertical orientation is observed for pyridine on the reconstructed Au(111) surface.[13] For the flat adsorption configuration, the permanent dipole moment of the pyridine molecule is almost parallel to the surface and the interaction occurs via the π-electrons of the aromatic ring, while in the vertically orientated pyridine adsorption structure, pyridine binds to the surface via its nitrogen atom.[13]

In this paper, a study of pH effects in pyridine adsorption on Au(111) at relative high bulk concentrations is presented together with the ramifications on electrooxidation of formate/formic acid.

Experimental

The Au(111) electrode (oriented better than 1°, MaTecK, Jülich, Germany) was flame annealed and checked for cleanliness and surface quality by cyclic voltammetry in 0.1 M H_2SO_4 (Merck, suprapur). After the removal of sulfate by thoroughly rinsing with water, the single crystal electrode was transferred to another electrochemical cell in a hanging meniscus configuration. Where possible, chemicals were obtained as suprapure quality from Merck (Darmstadt, Germany) and from Sigma-Aldrich as trace metal basis quality. For solution preparation and apparatus cleaning ultra-pure water (18.2 MΩ cm, TOC ≤ 3 ppb) was used. In all measurements the sum of formate and formic acid concentration was kept constant at 0.1 M whereas the pH was adjusted by addition of perchloric acid or sodium hydroxide, respectively. The conductivity was increased in most cases by addition of sodium perchlorate ($HClO_4$ + NaOH). Pyridine (≥99,9%, ChromasolPlus, Sigma-Aldrich) was used as obtained without further purification.

The electrochemical measurements were performed with a conventional three-electrode setup and a saturated mercury/mercurous sulfate electrode (SMSE) as reference electrode connected via a Haber–Lugging capillary. An Autolab PGSTAT182N potentiostat with Scan250 module was employed for all measurements. Temperature control was achieved by a water jacket enclosing the cell body. Potentials were corrected for *IR*-drop due to the strong change of electrolyte resistance. All measurements in this study were carried out at a temperature of 20°C.

Results and Discussion

First, adsorption properties of pyridine on Au(111) are described, before the influence of adsorbed pyridine on formic acid oxidation is presented. We focus on systematic trends for pyridine adsorption on a well-defined Au(111) surface as function of solution pH.

Adsorption properties of pyridine on Au(111).—Figure 1a depicts a typical cyclic voltammogram for Au(111) in 0.301 M $HClO_4$ + 0.3 M NaOH + 0.1 M pyridine at pH 7.2 and 100 mV s^{-1}. A broad peak P_{ad} between −1.2 and −1.0 V indicates adsorption of pyridine[13] on the reconstructed Au(111) surface in a flat configuration, where the π-electrons of the aromatic ring interact with the surface.[19,20] Orientation of pyridine changes at peak P_{up} around −0.6 V, where an upright configuration has been reported.[13] Pyridine is then bound to the (1 × 1) surface via its N atom. The relatively large charge density of around 20 μC cm^{-2} for P_{up} is related with a substantial shift of the potential of zero charge by −0.6 V.[13] Peak P_{up} is composed of several contributions giving rise to shoulders and spikes, especially for lower scan rates. However, in the following, these details shall not

*Electrochemical Society Member.
zE-mail: ludwig.kibler@uni-ulm.de

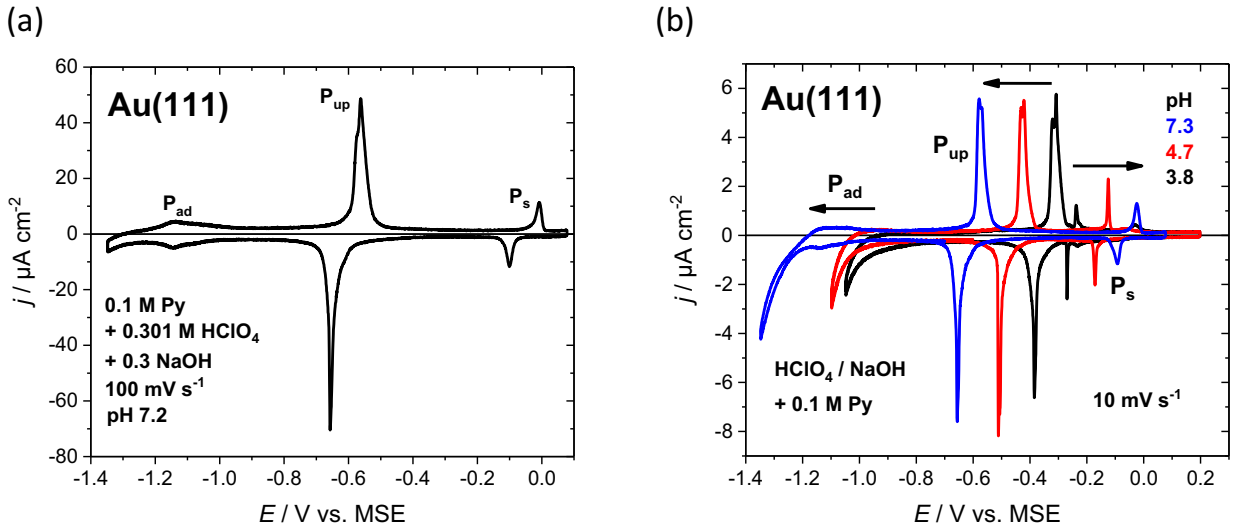

Figure 1. (a) Cyclic voltammogram for Au(111) in 0.301 M $HClO_4$ + 0.3 M NaOH + 0.1 M pyridine at pH 7.2 and a scan rate of 100 mV s^{-1}. (b) Series of selected cyclic voltammograms for Au(111) in ca. 0.3 M $HClO_4$ + ca. 0.3 M NaOH + 0.1 M pyridine at 10 mV s^{-1} for a wider range of pH values.

be taken into account, but rather the stability of various surface phases of pyridine shall be discussed. A further peak P_s close to 0 V (Figure 1a) corresponds to another phase transition were the adsorption of a second layer of pyridine had been suggested.[21] It will be shown below that process P_s is related to the presence of both pyridine and perchlorate. In any case, the anodic and cathodic parts of P_{up} and P_s show a marked peak-to-peak separation for the different scan directions.

In Figure 1b, a series of cyclic voltammograms for different pH values is shown. The various peaks P_{ad}, P_{up} and P_s indicating changes in the adsorption structures of pyridine on Au(111) are distinctly pH-dependent. For P_{ad} and P_{up} a shift toward more negative potentials for pH values increasing from 3.8 to 7.3 can be observed. However, for peak P_s the opposite behavior is observed. This process shifts to more positive potentials with increasing pH. For pH > 9 those two peaks are accompanied by the commencing surface oxidation of Au(111) and at pH 12 they are not present anymore. In all three cases, no further potential shifts have been observed for pH values higher than 6, where the solution contains pyridine in the unprotonated form ($pK_a = 5.23$).

A systematic series of measurements in a wide pH range has been performed in addition to the data given in Figure 1. From the positions of the different peaks, P_{ad}, P_{up} and P_s, a potential/pH diagram for pyridine adsorption on Au(111) has been derived (Figure 2). In general, cyclic voltammograms with a scan rate of 10 mV s^{-1} were used for the potentials of P_{up} and P_s. Higher scanrates were chosen to better identify P_{ad}, because pyridine adsorption overlaps with the hydrogen evolution reaction (HER). The potential/pH diagram in Figure 2 contains information about these voltammetric peaks for 25 experiments of pyridine adsorption on Au(111) at various pH values between 1 and 13. For the individual data points, "error bars" indicate the peak-to-peak separation for anodic and cathodic peaks of the individual processes.

Between the reversible potentials for the HER and the oxygen evolution reaction (OER), various stable phases for pyridine on Au(111) can be classified.

Phase I: Pyridine adsorbs in a flat orientation on the reconstructed surface and is bound mainly through the π-system of the aromatic ring. The coverage is around 0.06 ML[13] and DFT calculations suggest a certain small tilt angle of the molecule relative to the Au(111) surface.[22]

Phase II: After a gradual change from flat to vertical orientation which is related to shoulders and spikes within the main peak P_{up}, pyridine is now σ-bonded via the nitrogen to the Au(111) surface.[15] The coverage has increased to about 0.3 ML.[13] The relatively high peak charge density of P_{up} arises from a substantial shift in pzc.[13]

Phase III: The coverage and the orientation of pyridine only slightly change, while anion adsorption takes place and the Au(111) surface reconstruction is lifted.[23]

It is expected that the potentials of phase boundaries do not change with pH, because pyridine as neutral molecule does not involve the transfer of protons. The pH dependence of the peak potentials below pH 6 is assumed to be mostly connected to the lower concentration of unprotonated pyridine in solution. The diagram in Figure 2 for 0.1 M pyridine solutions thus reflects a concentration effect with slopes dE/dpH for P_{ad}: −0.12 to 0.13 V dec^{-1}, P_{up}: −0.18 V dec^{-1} and

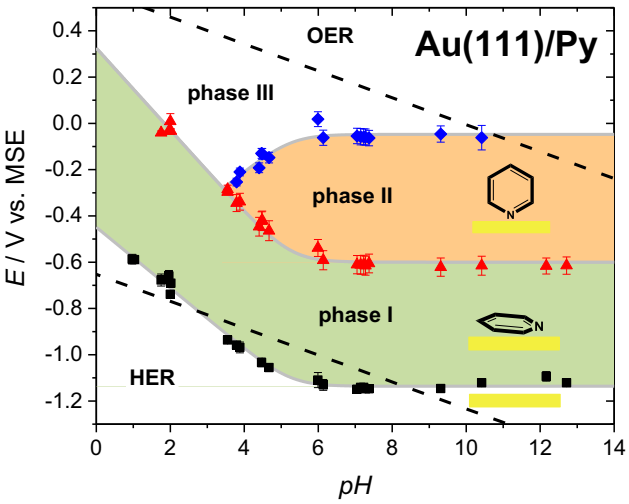

Figure 2. Potential/pH diagram of the voltammetric features for Au(111) in x M $HClO_4$ + y M NaOH + 0.1 M pyridine. Potentials are extracted mostly from 10 mV s^{-1} cyclic voltammetric measurements and from higher scan rates where hydrogen evolution overlaps. The error bars indicate the full potential range between anodic and cathodic peaks for the individual electrochemical processes. The broken lines follow the reversible potentials for water electrolysis, i. e. for the oxygen and hydrogen evolution reactions, OER and HER, respectively. Three main adsorbed phases of pyridine on Au(111) are indicated in the potential regimes between voltammetric peaks.

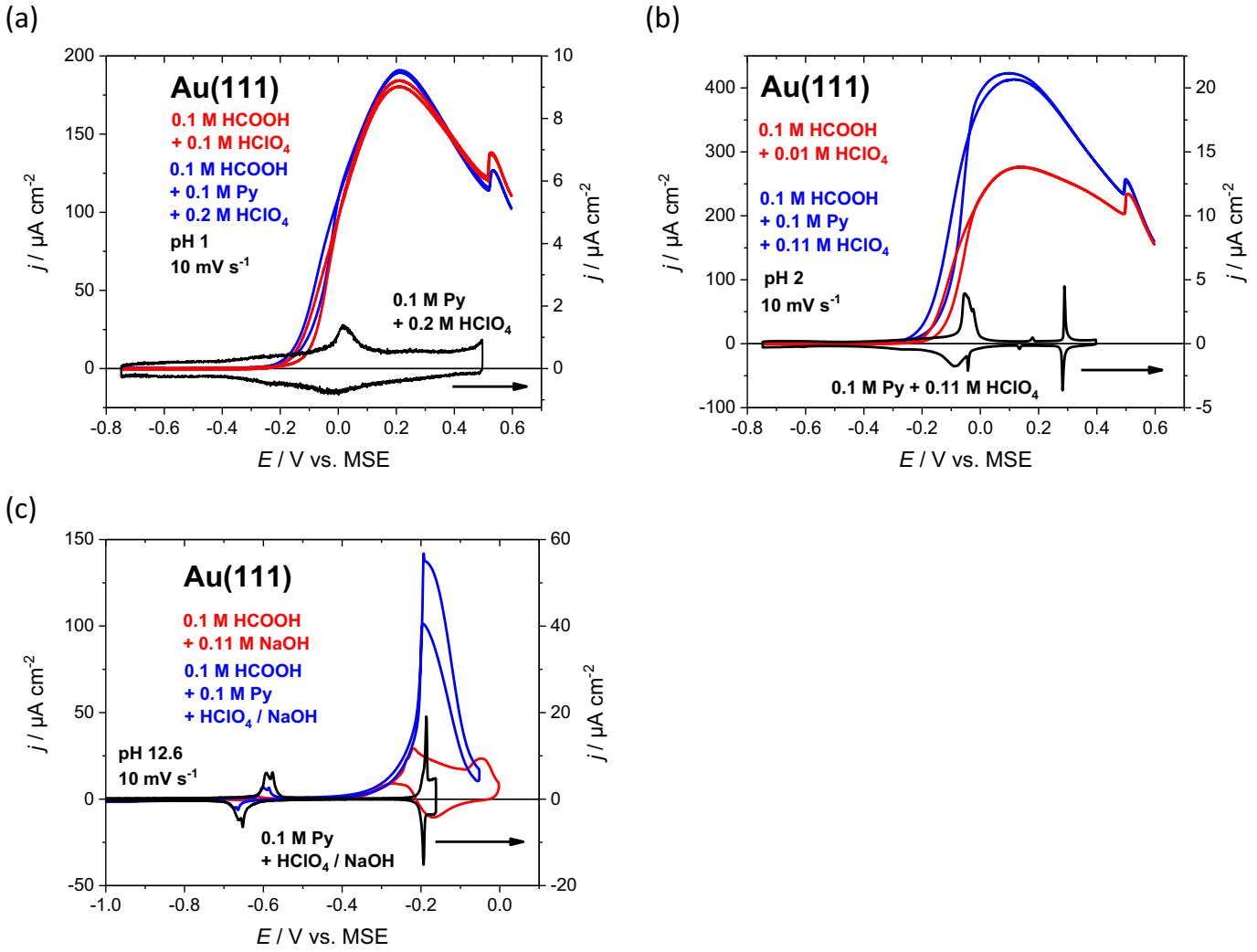

Figure 3. Cyclic voltammograms illustrating the effect of pyridine on the formic acid oxidation at low and high pH values. (a) Current potential curves for formic acid oxidation at Au(111) in 0.1 M HCOOH + 0.1 M $HClO_4$ (red curve) and with the addition of pyridine in 0.1 M HCOOH + 0.1 M pyridine + 0.2 M $HClO_4$ (blue curve) at pH 1 and a scan rate of 10 mV s^{-1}. The cyclic voltammogram of the base system without HCOOH for Au(111) in 0.1 M pyridine + 0.2 M $HClO_4$ is depicted in black. (b) Current potential profiles for formic acid oxidition at Au(111) in 0.1 M HCOOH + 0.01 M $HClO_4$ (red curve) and with the addition of pyridine in 0.1 M HCOOH + 0.1 M pyridine + 0.11 M $HClO_4$ (blue curve) at pH 2 and 10 mV s^{-1} scan rate. The cyclic voltammogram of Au(111) in 0.1 M pyridine + 0.11 M $HClO_4$ (black curve) exhibits pyridine related peaks. (c) Current potential curves for formic acid oxidation on Au(111) in 0.1 HCOOH + 0.11 M NaOH (red curve) and in 0.1 HCOOH + 0.1 M pyridine + 0.32 $HClO_4$ + 0.52 NaOH (blue curve) at pH ~12–13 and a scan rate of 10 mV s^{-1}. Cyclic voltammogram of the base system without formic acid is given for Au(111) in 0.1 M pyridine + 0.3 M $HClO_4$ + 0.31 NaOH (black curve, pH 12.6).

P_s: +0.13 V dec^{-1}. Knowledge of this behavior is crucial for understanding the electrooxidation of formic acid in presence of pyridine in the pH range studied.

Influence of adsorbed pyridine on FAO.—The effect of pyridine on the electrocatalytic formic acid oxidation is very strongly dependent on pH, as will be discussed in the following and as shown in Figures 3–5. Already before adding pyridine to the system, the formic acid oxidation shows a distinct intrinsic pH influence (red curves in Figures 3–5).[9,10] The maximum current density of the bell-shaped oxidation peak increases with increasing pH until an activity plateau is reached for pH > 5. Different pH regimes of enhancement can be identified, depending on the effect of 0.1 M pyridine (Py) on HCOOH oxidation. It should be noticed that adequate amounts of $HClO_4$ and/or NaOH were also added together with pyridine in order to keep the solution pH constant for sake of comparison (blue curves in Figures 3–5). This has other consequences, because anion effects play a central role in formic acid oxidation on Au(111) with and without adsorbed pyridine, as will be discussed below. For very low and very high pH values the enhancement effect of pyridine is much less pronounced than for the intermediate region 2 < pH < 10 (see below). At first, the two former regions shall be discussed, before the strong enhancement is addressed.

pH 1: Addition of 0.1 M pyridine shows little effect on HCOOH oxidation (Figure 3a, blue curve; red curve without pyridine for comparison). It seems that the pyridinium cation, which is dominating in solution does not interact strongly with the Au(111) surface. The black curve in Figure 3a shows a cyclic voltammogram for Au(111) in 0.2 M $HClO_4$ + 0.1 M pyridine, with no characteristic pyridine peaks as for higher pH values. The surface reconstruction is lifted around 0 V. The molar fraction of unprotonated pyridine is quite small and therefore shows little effect and no characteristic pyridine peaks under these conditions. Essentially, the well-known bell-shaped formic acid oxidation curve including the characteristic step-up in current due to a phase transition within the strongly bound formate adlayer[11] at around 0.52 V is observed with and without pyridine in solution (red and blue curves in Figure 3a). The slight hysteresis in electrocatalytic activity between −0.2 and −0.05 V is caused by reconstruction phenomena,[24] the reconstructed surface being less active for formic acid oxidation than the (1 × 1) surface.

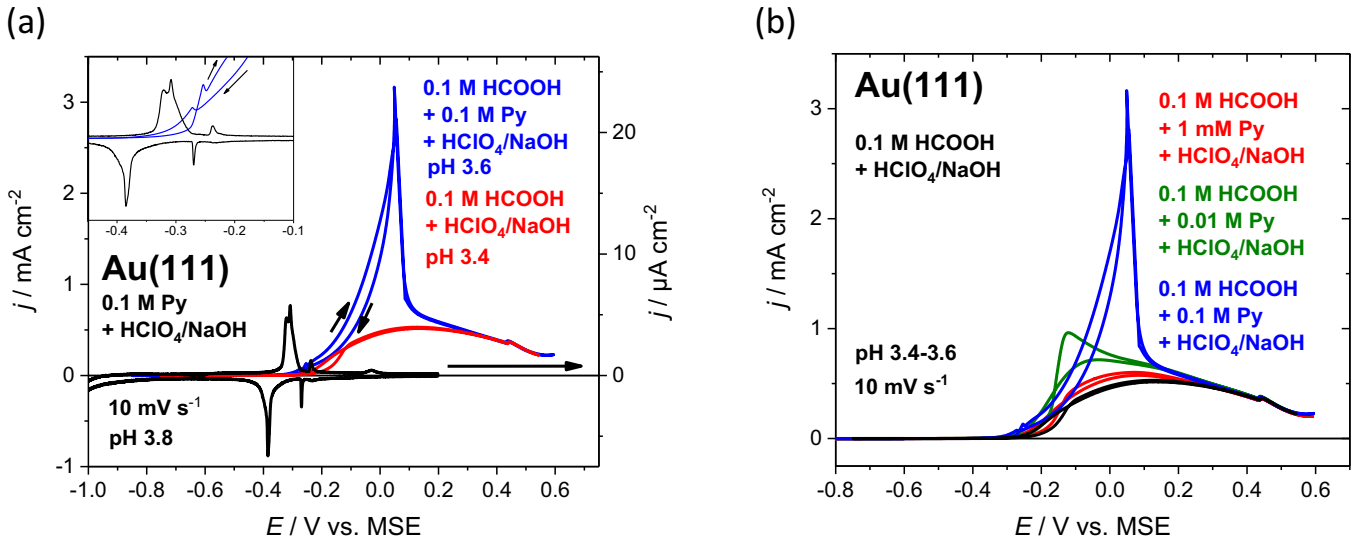

Figure 4. (a) Current potential curves for formic acid oxidation on Au(111) in 0.1 M HCOOH + 0.125 M NaOH + 0.075 M $HClO_4$ (pH 3.4, red curve) and enhanced reaction for Au(111) in 0.1 M pyridine + 0.1 M HCOOH + 0.05 M $HClO_4$ + 0.1 M NaOH (pH 3.6, blue curve) at a scan rate of 10 mV s^{-1}. The black curve displays the behavior of the base system Au(111) in 0.1 M pyridine + 0.3 M $HClO_4$ + 0.2 M NaOH. (b) Cyclic voltammograms for formic acid oxidation on Au(111) in 0.1 M HCOOH + 0.075 $HClO_4$ + 0.125 M NaOH (black curve, pH 3.4) and with the addition of pyridine in 0.1 M HCOOH + 1 mM pyridine + 0.051 M $HClO_4$ + 0.1 M NaOH (red curve, pH 3.6), in 0.1 M HCOOH + 0.01 M pyridine + 0.06 M $HClO_4$ + 0.1 M NaOH (green curve, pH 3.6) and in 0.1 M HCOOH + 0.1 M pyridine + 0.1 M $HClO_4$ + 0.2 M NaOH (blue curve, pH 3.6) at 10 mV s^{-1}.

pH 2: The onset of formic acid oxidation is only slightly shifted toward more negative potentials after adding 0.1 M pyridine to the solution (red and blue curves in Figure 3b). In this low potential region, the electrocatalytic enhancement is quite pronounced but diminishes with increasing potential until the oxidation curves merge at potentials above 0.5 V, where the presence of the characteristic current kink suggests that strongly bound formate dominates the interfacial adlayer. This observation indicates that adsorbed pyridine is displaced by strongly bound formate at sufficiently high potentials. The current density reaches a maximum of more than 400 µA cm^{-2} at a potential where pyridine itself adopts the vertical orientation on Au(111). The base system Au(111) in 0.1 M pyridine + 0.11 M $HClO_4$ yields a peak at −0.05 V corresponding to the formation of the vertical pyridine structure. However, in the presence of HCOOH there is no clear indication of this phase transition within the pyridine adlayer. A closer inspection of the electrocatalytic current densities with and without pyridine shows an enhancement of about 50% in the potential region between −0.1 V and 0.2 V, which decreases gradually for increasing electrode potentials (Figure 3b). It is assumed that a mixed pyridine + formate adlayer is formed with gradual increase in anion coverage at $E > 0.2$ V. At lower potentials, negative of peak P_{up}, the electrocatalytic enhancement is clearly larger than 50%, which shows that the flat orientation of pyridine with the low coverage reveals a real boosting effect under these experimental conditions.

It can be summarized (i) that pyridine in the flat orientation promotes the FAO more strongly than the vertical orientation and (ii) that coadsorption of anions diminishes the boosting effect of adsorbed pyridine (specific adsorption of spectator species leads to blocking of active centers already in the absence of pyridine).[11] For pH 2, the molar fraction of unprotonated pyridine is around 10^{-3} leading to an effective concentration of 0.1 mM, which is enough to enhance the electrocatalytic activity by 50% at the current maximum.

pH 12: The oxidation reaction commences in the same potential region after adding 0.1 M pyridine (red and blue curve in Figure 3c). In this case, the vertical orientation of pyridine is already present and the electrocatalytic activity is at first only slightly increased. Sharp oxidation peaks with substantially increased current densities occur for both scan directions around −0.2 V. It is supposed that OH adsorbs on Au(111) above −0.2 V (see black curve in Figure 3c). Adsorbed pyridine shifts surface oxidation toward slightly more positive potentials, which allows for a FAO enhancement in a narrow potential region. This means that adsorbed pyridine unmasks the intrinsic FAO activity of Au(111) by a small shift of OH adsorption toward more positive potentials.

The intermediate pH region (2 < pH < 10) shows a dramatic enhancement of formic acid oxidation after adding 0.1 M pyridine (blue curves in Figures 4a+4b and 5a–5c). In these cases, pyridine is in its vertical adsorption configuration already, when the oxidation of formic acid commences. For pH values below pK_a of pyridinium (5.23), i.e. for low concentrations of unprotonated pyridine, there are relatively sharp FAO current maxima at about 0.05 V before the enhancement breaks down at positive potentials, where the boosting effect of pyridine vanishes and curves with and without pyridine merge (blue and red curves in Figures 4a+4b). It is also observed from the inset of Figure 4a that the phase formed positive of peak P_s at −0.25 V is less active than the vertical pyridine phase formed at peak P_{up}, since the oxidation current density decreases with increasing potential. It can be concluded that FAO activity is influenced by the presence of both pyridine and perchlorate, which gives rise to process P_s. While it typically belongs to the weakly adsorbing anions, it is surprising that perchlorate lowers the electrocatalytic activity in alliance with adsorbed pyridine.

Though the orientation and the surface coverage of adsorbed pyridine on Au(111) are strongly dependent on pH and electrode potential (Figure 2), the stability range of the individual surface phases can be shifted by varying the pyridine concentration by ca. 0.15 V dec^{-1}.[14] Since the flat pyridine configuration was identified to be more active than the vertical orientation (see above), it was attempted to shift peak P_{up} toward more positive potentials by lowering the pyridine concentration.

The dependence of the formic acid oxidation on pyridine concentration is displayed in Figure 4b at 10 mV s^{-1} and at an almost constant pH of 3.5 ± 0.1. In contrast to 0.1 M pyridine, there is no sharp FAO current maximum anymore with 10 mM pyridine (Figure 4b, green curve). Indeed, as expected for the flat pyridine adlayer, in a narrow potential range between −0.2 V and −0.1 V the FAO activity is larger with 10 mM than with 0.1 M. If the pyridine concentration is too low, e.g. 1 mM, the enhancement effect is negligible (red curve). In all cases, pyridine seems to be displaced by strongly bound formate

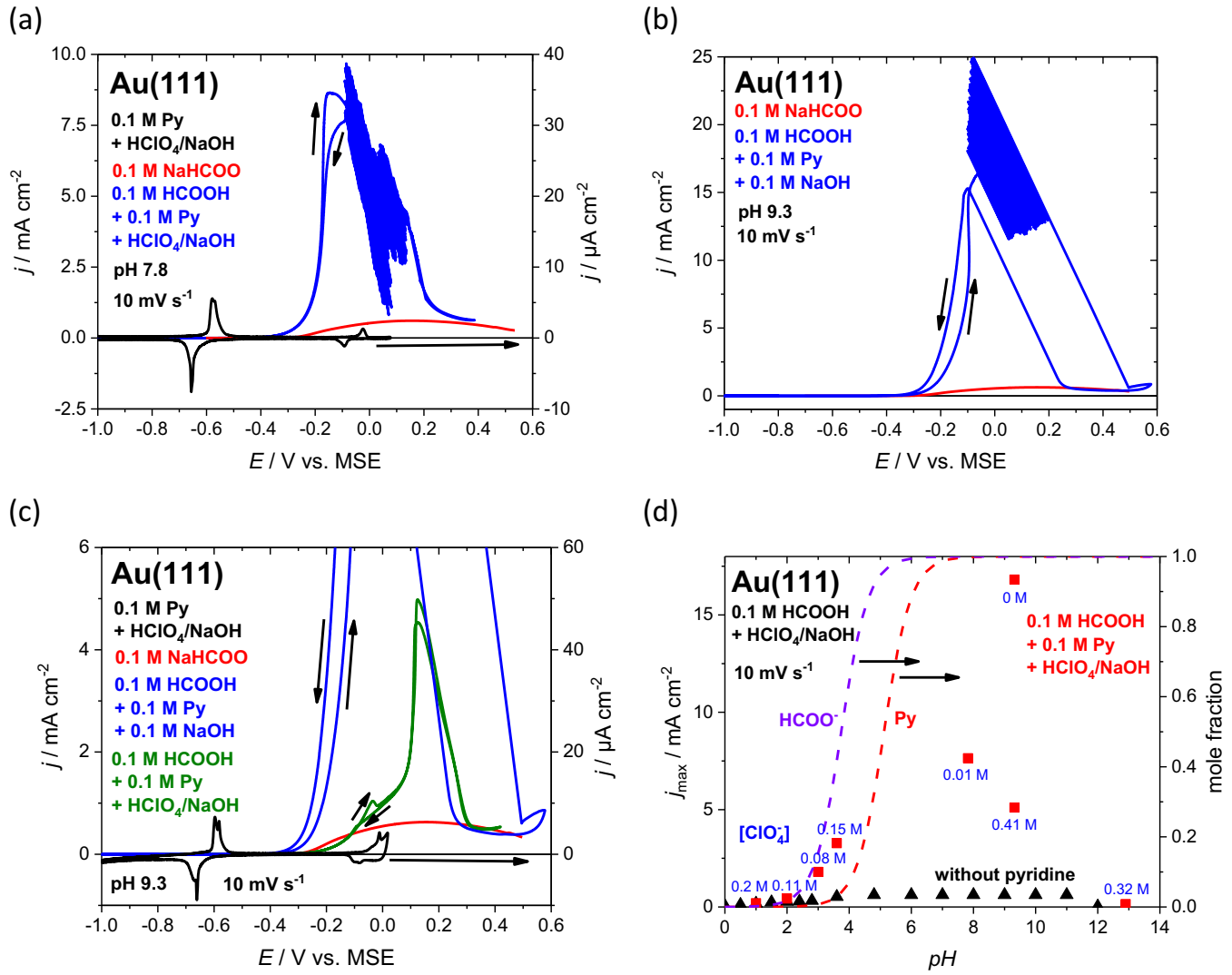

Figure 5. (a) Current potential curves for formic acid oxidation on Au(111) in 0.1 M NaHCOO (red curve) and in 0.1 M pyridine + 0.1 M HCOOH + 0.013 M $HClO_4$ + 0.117 NaOH (blue curve, pH 7.2) at 10 mV s^{-1}. The base curve of Au(111) in 0.1 M pyridine + 0.301 M $HClO_4$ + 0.3 M NaOH is depicted in black. (b) Cyclic voltammogramm of Au(111) in 0.1 M NaHCOO (red curve) and in 0.1 M HCOOH + 0.1 M pyridine + 0.1 M NaOH (blue curve) at 10 mV s^{-1}. (c) Same as (b) with curves for solution of 0.1 M pyridine + 0.1 M HCOOH + 0.41 $HClO_4$ + 0.51 NaOH and base curve in 0.1 M pyridine + 0.29 M $HClO_4$ + 0.29 NaOH (black curve, pH 9.3). (d) Maximum current densities vs. pH extracted from cyclic voltammograms for Au(111) in 0.1 M HCOOH/NaHCOO + $HClO_4$/NaOH (black triangles) and with additional 0.1 M pyridine (red squares). Blue text at red points indicates the concentration of perchlorate in solution. The mole fraction of unprotonated pyridine (red curve) and formate (purple curve) is indicated by dashed lines.

at $E > 0.2$ V and the current–potential profiles become independent on pyridine concentration.

The catalytic effect of adsorbed pyridine in this intermediate pH region is manifold: (i) Pyridine is able to shift the adsorption of strongly bound formate to more positive potentials. Since strongly bound formate blocks reactive sites, the presence of pyridine is advantageous. (ii) Pyridine represents a strong molecular dipole, which may help to bring weakly bound formate species into the reactive configuration and not to the strongly bound bidentate adsorption state. (iii) Pyridine can act as a strong base to accept protons generated during the formic acid oxidation reaction. (iv) Pyridine might interact directly with reactive intermediates in a catalytic step.

It is clear that electrochemical measurements alone are not sufficient to identify the catalytic role of pyridine. While further spectroscopic and theoretical studies are needed to elucidate the reaction mechanism for FAO on pyridine-modified Au(111), the present electrochemical study highlights the effects of pH and electrode potential in a systematic way. So far, the suppression of specific adsorption of anions by adsorbed pyridine in a certain potential region is supposed to be most important.

At pH values greater than the pK_a of pyridinium the appearance of the current potential curves changes dramatically. The current maxima in Figures 5a+5b for FAO are less sharp than for lower pH values, but the observed current densities are exceedingly high. In addition, characteristic oscillations occur near the current density maxima. Similar oscillations are known for formic acid oxidation on other noble metal surfaces, especially for Pt electrodes.[25,26]

The results for enhancement in formic acid oxidation gathered over the wide pH range suggest that not only the absolute concentration of pyridine but also the molar ratio of both formate and pyridine is relevant. This is substantiated by the cyclic voltammograms in Figure 4b, where the pyridine concentration is varied at constant pH and constant formic acid concentration. For high pyridine concentrations the sharp peak (see above) is present which diminishes for lower concentrations.

$$r = \frac{[HCOO^-]}{[\text{pyridine}]} \qquad [1]$$

Accordingly, the ratio r of free formate and pyridine concentration (Eq. 1) changes over pH and three regions can be identified (total

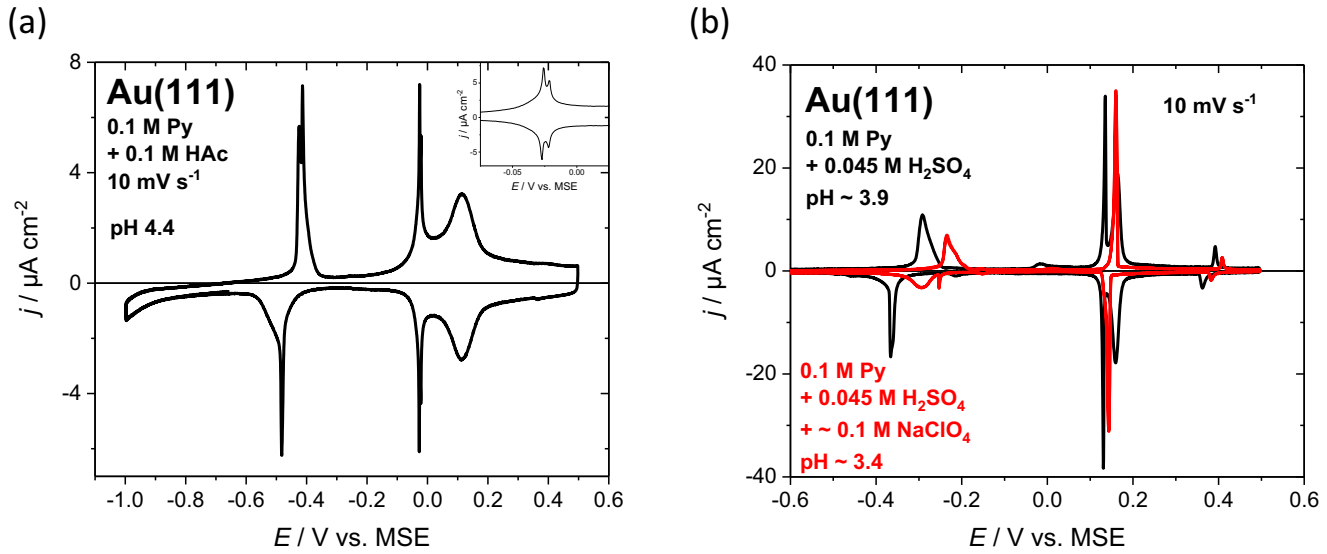

Figure 6. Current potential curves for different anions with pyridine. (a) Cyclic voltammograms for Au(111) in 0.1 M pyridine + 0.1 M acetic acid (pH 4.4). (b) Cyclic voltammograms of Au(111) in 0.1 M pyridine + 0.045 M H_2SO_4 (pH ~3.9, black curve) and with additional ~0.1 M $NaClO_4$ (pH ~3.4, red curve).

concentrations are 0.1 M). (i, $r > 25$) At pH values far below the pK_a of HCOOH the concentrations of both unprotonated pyridine and formate in solution are small (e.g. at pH 2), which results in smooth curves and an enhancement over a wide potential range. (ii, $5 < r < 25$) At pH values near the pK_a of HCOOH the absolute concentration of formate is already noticeably higher and the positive limit of the enhancement is shifted toward more negative potentials due to formate adsorption. (iii, $1 \leq r \leq 5$) At pH values close to or higher than pK_a of pyridinium, the absolute concentrations of pyridine and formate are high and their ratio is close to equimolar. The reaction is enhanced up to more positive potentials.

An overview on boosting reaction kinetics by pyridine is given in Figure 5d, where maximum current densities for formic acid oxidation with and without pyridine present are plotted as a function of pH. The formic acid oxidation without pyridine exhibits rising current densities for pH values lower than the pK_a of formic acid followed by an activity plateau until pH 11. At pH > 12 the activity breaks down due to competing adsorption of hydroxide on Au(111) (see also Figure 3c). In the presence of pyridine the enhancement is obvious from pH 3 to 10 and vanishes for very high pH values (poor activity at pH 13). In Figure 5d, the concentration of perchlorate is indicated in blue next to the data points. Especially for pH 9 a dramatic suppressing effect of this weakly adsorbing anion is obvious. At the same time, changes in the base electrolyte composition lead to the disappearance of the oscillations, an effect that has been observed for related systems.[27]

Role of adsorbing anions.—In addition to the remarkable boosting effect of pyridine on formic acid oxidation, it is clear that coadsorbed anions play a central role in this electrocatalytic system. Not only the concentration of perchlorate influences the maximum electrocatalytic currents (Figure 5d), also adsorption of strongly bound formate at positive potentials disables the enhancement so that currents with and without pyridine become identical (Figures 3–5). Unfortunately, the study of formate adsorption is hampered by the oxidation reaction itself. For this reason the behavior of other oxyanions in addition to adsorbed pyridine will be addressed in the following.

Acetate as carboxylate is chosen because its adsorption behavior is assumed to be very similar to that of formate (spectator species in FAO). Figure 6a shows a cyclic voltammogram of Au(111) in 0.1 M HAc + 0.1 M pyridine (pH 4.4). The process of the orientational change in the pyridine layer at −0.45 V is unaffected by the presence of acetate. At a potential of −0.03 V a "double-spike" (Figure 6a, inset) emerges followed by a broad peak at 0.11 V. These processes have a remarkably low peak-to-peak separation of less than 10 mV, the "double-spike" at −0.03 V shows a split of 5 mV. These processes are associated to acetate adsorption on Au(111) and correspond to a total charge density of about 70 µC cm^{-2}. The onset of acetate adsorption is slightly hindered by the vertical pyridine structure. At the sharp spike (around 0 V) the adsorbing acetate seems to break up the pyridine structure. At more positive potentials, coadsorption and/or the advancing replacement of adsorbed pyridine occur. A comparison of the adsorption behavior of acetate with the findings for formate adsorption during formic acid oxidation at pH 3.6 (see above and Figure 4a) provides evidence for shifting anion adsorption toward slightly more positive potentials by adsorbed pyridine, which represents an essential part of the enhancing effect. Once the pyridine structure breaks down due to anion (co)adsorption at positive potentials, the enhancement vanishes.

Sulfate represents another strongly adsorbing oxyanion. In comparison to acetate, it shows a very similar effect on the current–potential curve of Au(111) in 0.1 M pyridine (Figure 6b, black curve). The addition of perchlorate to the electrolyte (red curve) will be discussed below. Sulfate exhibits a combination of sharp spike at 0.13 V and broader adsorption peak at 0.16 V. The peak P_{up} for the formation of the vertical pyridine structure at −0.29 V displays a clearly different shape compared to acetate and perchlorate containing electrolytes. In addition, a second spike at 0.39 V appears. This second spike is easily related with the formation of the well-known $(\sqrt{7} \times \sqrt{3})$R19.1° structure of sulfate on Au(111).[28] Also in this case, adsorbed pyridine is displaced by specifically adsorbed anions.

Hydroxide is another example of a strongly adsorbing anion, which is especially important for surface oxidation of metals at positive potentials in aqueous electrolytes. For pH 12 ($[OH^-] \approx 0.01$ M), a spike is observed in the commencing OH adsorption at a potential of −0.195 V (Figure 3c, black curve).

Surprisingly, voltammograms for pyridine adsorption with strongly adsorbing anions present are very similar to that of pyridine adsorption in the presence of perchlorate. In contrast to the anions discussed above, perchlorate is considered to be weakly adsorbing and is therefore used in the majority of studies of pyridine adsorption.[13,14,21,23] Figure 3b shows the current potential curve for Au(111) in 0.1 M pyridine + 0.11 M $HClO_4$ (black curve). Pyridine adsorption occurs at −0.65 V and the orientational change takes place around −0.05 V at peak P_{up}. The other two processes at 0.15 V and 0.28 V were only observed in the region close to pH 2. Remarkably, the sharp spike at 0.28 V exhibits a very small peak-to-peak

separation, which is also seen for the specifically adsorbing anions (see above). The narrow pH range for the occurrence of these two voltammetric features is likely linked to the extreme ratio of free pyridine and perchlorate. Under these conditions perchlorate seems to interact with the pyridine covered Au(111) surface in a way very similar to the strongly adsorbing anions.

The unique adsorption behavior of perchlorate is also evident for mixed electrolytes. The red curve in Figure 6b is obtained for Au(111) in 0.1 M pyridine + 0.1 M $NaClO_4$ + 0.045 M H_2SO_4. A significantly altered behavior for the adsorption of sulfate compared to the measurement without perchlorate is observed (compare black curve in Figure 6b). The sharp spike followed by further adsorption merges into a single sharp peak at a potential of 0.15 V with noticeable peak-to-peak separation. This significant change in the adsorption behavior by perchlorate points to surprisingly strong interactions of perchlorate with the pyridine adlayer. Furthermore, it is in accordance with the observed strongly decreased current for formic acid oxidation in the presence of perchlorate (Figure 5c). Although perchlorates are prone to chloride contamination we believe that this is a genuine effect of perchlorate as no accumulation effects caused by chloride adsorption have been observed.

Conclusions

The adsorption of pyridine on well-ordered Au(111) electrodes shows a distinct pH dependence. Peak potentials of P_{ad} for pyridine adsorption, P_{up} for the change in adsorption configuration from flat to vertical, and P_s for coadsorption of perchlorate anions have been used to compose a potential/pH diagram for pyridine adsorbed on the Au(111) surface. This is helpful in gaining a better knowledge of the adsorption of pyridine molecules in general. Various stability regions of adsorbed pyridine phases are classified.

Adsorbed pyridine can enhance the oxidation of formic acid on Au(111) significantly, especially at $2 < pH < 10$. The flat orientation of pyridine shows a greater boosting effect than the vertical configuration. This fundamental study of a simple electrocatalytic process demonstrates the importance of adsorption processes in understanding electrocatalytic reactions and gives examples of relations between adsorption structure and reactivity: the adsorption processes of reactants, intermediates, anions, spectator species, and molecular promoters play a central role in formic acid oxidation on gold in presence of pyridine.

The boosting effect of pyridine is related to a shift of strongly adsorbed formate toward more positive potentials. In particular, the adsorbed pyridine seems to be advantageous for bringing formate species into the reactive configuration.

The behavior of pyridine and its enhancing effect in formic acid oxidation is important for understanding the properties of other molecular promotors, such as 4-mercaptopyridine or other nitrogen-containing organic molecules.

Acknowledgments

Support by the Fonds der Chemischen Industrie is greatly acknowledged.

ORCID

Ludwig A. Kibler https://orcid.org/0000-0003-1152-1445

References

1. D. M. Kolb, "Electrochemical Surface Science" *Angew. Chem. Int. Ed.*, **40**, 1162 (2001).
2. D. M. Kolb, "Electrochemical surface science: past, present and future" *J. Solid State Electrochem.*, **15**, 1391 (2011).
3. R. R. Adžić, A. V. Tripković, and W. E. O'Grady, "Structural effects in electrocatalysis" *Nature*, **296**, 137 (1982).
4. R. R. Adžić, D. N. Simić, A. R. Despić, and D. M. Dražić, "Electrocatalysis by foreign metal monolayers–oxidation of formic acid on platinum" *J. Electroanal. Chem.*, **65**, 587 (1975).
5. R. R. Adžić, D. N. Simić, A. R. Despić, and D. M. Dražić, "Electrochemical oxidation of formic acid at noble metals: catalytic effects of foreign metal monolayers" *J. Electroanal. Chem.*, **80**, 81 (1977).
6. A. Cuesta, G. Cabello, F. W. Hartl, M. Escudero-Escribano, C. Vaz-Dominguez, L. A. Kibler, M. Osawa, and C. Gutierrez, "Electrooxidation of Formic Acid on Gold: an ATR-SEIRAS Study of the Role of Adsorbed Formate" *Catal. Today*, **202**, 79 (2013).
7. L. A. Kibler, A. M. El-Aziz, R. Hoyer, and D. M. Kolb, "Tuning Reaction Rates by Lateral Strain in a Palladium Monolayer" *Angew. Chem. Int. Ed.*, **44**, 2080 (2005).
8. J. Zhang, M. B. Vukmirovic, Y. Xu, M. Mavrikakis, and R. R. Adzic, "Controlling the Catalytic Activity of Platinum-Monolayer Electrocatalysts for Oxygen Reduction with Different Substrates" *Angew. Chem. Int. Ed.*, **44**, 2132 (2005).
9. A. Abdelrahman, J. M. Hermann, and L. A. Kibler, "Electrocatalytic Oxidation of Formate and Formic Acid on Platinum and Gold: Study of pH Dependence with Phosphate Buffers" *Electrocatal.*, **8**, 509 (2017).
10. S. Brimaud, J. Solla-Gullón, I. Weber, J. M. Feliu, and R. J. Behm, "Formic Acid Electrooxidation on Noble-Metal Electrodes: Role and Mechanistic Implications of pH, Surface Structure, and Anion Adsorption" *ChemElectroChem*, **1**, 1075 (2014).
11. L. A. Kibler and M. Al-Shakran, "Adsorption of Formate on Au(111) in Acid Solution: Relevance for Electro-Oxidation of Formic Acid" *J. Phys. Chem. C*, **120**(29), 16238 (2016).
12. A. Hamelin, "Coadsorption of sulfate ions and pyridine on the (111), (110) and (100) faces of gold" *J. Electroanal. Chem.*, **144**, 365 (1983).
13. L. Stolberg, S. Morin, J. Lipkowski, and D. E. Irish, "Adsorption of pyridine at the Au(111)-solution interface" *J. Electroanal. Chem.*, **307**, 241 (1991).
14. S. Iqbal, S. Wezisla, N. Podgaynyy, and H. Baltruschat, "Pyridine on Au(111): A frictional transition controlled by electrochemical potential" *Electrochim. Acta*, **186**, 427 (2015).
15. W.-B. Cai, L.-J. Wan, H. Noda, Y. Hibino, K. Ataka, and M. Osawa, "Orientational Phase Transition in a Pyridine Adlayer on Gold(111) in Aqueous Solution Studied by in Situ Infrared Spectroscopy and Scanning Tunneling Microscopy" *Langmuir*, **14**, 6992 (1998).
16. P. Hébert, A. Le Rille, W. Q. Zheng, and A. Tadjeddine, "Vibrational spectroscopic study of the adsorption of pyridine at the Au(111)-electrolyte interface by in situ difference frequency generation" *J. Electroanal. Chem.*, **447**, 5 (1998).
17. M. Hoon-Khosla, W. R. Fawcett, A. Chen, J. Lipkowski, and B. Pettinger, "A SNIFTIRS study of the adsorption of pyridine at the Au(111) electrode–solution interface" *Electrochim. Acta*, **45**, 611 (1999).
18. Y. Ikezawa, T. Sawatari, and H. Terashima, "In situ FTIR study of pyridine adsorbed on Au(111), Au(100) and Au(110) electrodes" *Electrochim. Acta*, **46**, 1333 (2001).
19. G. Andreasen, M. E. Vela, R. C. Salvarezza, and A. J. Arvia, "Dynamics of Pyridine Adsorption on Gold(111) Terraces in Acid Solution from in-Situ Scanning Tunneling Microscopy under Potentiostatic Control" *Langmuir*, **13**, 6814 (1997).
20. D. Mollenhauer, N. Gaston, E. Voloshina, and B. Paulus, "Interaction of pyridine derivatives with a gold(111) surface as a model for adsorption to large nanoparticles" *J. Phys. Chem. C*, **117**, 4470 (2013).
21. J. F. Li, Y. J. Zhang, A. V. Rudnev, J. R. Anema, S. B. Li, W. J. Hong, P. Rajapandiyan, J. Lipowski, and Z. Q. Tian, "Electrochemical shell-isolated nanoparticle-enhanced Raman spectroscopy: correlating structural information and adsorption processes of pyridine at the Au(hkl) single crystal/solution interface" *J. Am. Chem. Soc.*, **137**, 2400 (2015).
22. K. Tonigold and A. Gross, "Adsorption of small aromatic molecules on the (111) surfaces of noble metals: A density functional theory study with semiempirical corrections for dispersion effects" *J. Chem. Phys.*, **132**, 224701 (2010).
23. S. Wu, J. Lipkowski, O. M. Magnussen, B. M. Ocko, and T. Wandlowski, "The driving force for $(p \times \sqrt{3}) \leftrightarrow (1 \times 1)$ phase transition of Au(111) in the presence of organic adsorption: a combined chronocoulometric and surface X-ray scattering study" *J. Electroanal. Chem.*, **446**, 67 (1998).
24. D. M. Kolb, "Reconstruction phenomena at metal-electrolyte interfaces" *Prog. Surf. Sci.*, **51**, 109 (1996).
25. P. Strasser, M. Lübke, F. Raspel, M. Eiswirth, and G. Ertl, "Oscillatory instabilities during formic acid oxidation on Pt(100), Pt(110) and Pt(111) under potentiostatic control I. Experimental." *J. Chem. Phys.*, **107**, 979 (1997).
26. G. Samjeské and M. Osawa, "Current Oscillations during Formic Acid Oxidation on a Pt Electrode: Insight into the Mechanism by Time-Resolved IR Spectroscopy" *Angew. Chem. Int. Ed.*, **44**, 5694 (2005).
27. B. E. Kumara Swamy, Ch. Vannoy, J. Maye, F. Kamali, D. Huynh, B. Britt Little II, and M. Schell, "Potential oscillations in formic acid oxidation in electrolyte mixtures: Efficiency and stability" *J. Electroanal. Chem.*, **625**, 69 (2009).
28. O. M. Magnussen, J. Hageböck, J. Hotlos, and R. J. Behm, "In-situ STM observations of a Disorder-Order Phase Transition in Bisulfate Adlayers on Au(111)" *Faraday Discuss.*, **94**, 329 (1992).